Geophysical Research Letters

RESEARCH LETTER
10.1029/2025GL115073

Giant Submarine Landslide on the East Antarctic Margin During the Plio-Pleistocene

Xiaoxia Huang[1], Laura De Santis[2], German Leitchenkov[3], Carlota Escutia[4], Flavio Accaino[2], Morelia Urlaub[5], and Robert M. McKay[6]

[1]Institute of Deep-Sea Science and Engineering, Chinese Academy of Sciences, Sanya, China, [2]National Institute of Oceanography and Applied Geophysics, OGS, Trieste, Italy, [3]All Russia Scientific Research Institute for Geology and Mineral Resources of the Ocean, St. Petersburg, Russia, [4]Instituto Andaluz de Ciencias de la Tierra, CSIC-Univ. de Granada, Armilla, Spain, [5]GEOMAR Helmholtz Centre for Ocean Research Kiel, Kiel, Germany, [6]Victoria University of Wellington, Wellington, New Zealand

Key Points:

- A giant submarine landslide complex is the first to be discovered on the East Antarctic margin, adjacent to the Wilkes Subglacial Basin
- Timing of slope failure potentially can be linked to the Pliocene-Pleistocene glacial variance
- Submarine landslide failure processes are influenced by sediment deposition, weak layers, and fluid or gas presence

Supporting Information:

Supporting Information may be found in the online version of this article.

Correspondence to:

X. Huang,
huangxx@idsse.ac.cn

Citation:

Huang, X., De Santis, L., Leitchenkov, G., Escutia, C., Accaino, F., Urlaub, M., & McKay, R. M. (2025). Giant submarine landslide on the East Antarctic margin during the Plio-Pleistocene. *Geophysical Research Letters*, *52*, e2025GL115073. https://doi.org/10.1029/2025GL115073

Received 5 FEB 2025
Accepted 3 JUN 2025

Author Contributions:

Conceptualization: Xiaoxia Huang
Formal analysis: Xiaoxia Huang
Funding acquisition: Xiaoxia Huang
Investigation: Xiaoxia Huang
Methodology: Xiaoxia Huang
Project administration: Xiaoxia Huang
Software: Xiaoxia Huang
Validation: Xiaoxia Huang
Visualization: Xiaoxia Huang
Writing – original draft: Xiaoxia Huang
Writing – review & editing: Xiaoxia Huang, Laura De Santis, German Leitchenkov, Carlota Escutia, Flavio Accaino, Morelia Urlaub, Robert M. McKay

Abstract A giant submarine landslide complex is reported on the George V margin of East Antarctic continental rise. Such landslides are imaged on seismic profiles that display evidence of basal glide planes and headwall scarps. A longitudinal seismic transect, and correlation to nearby drill sites suggest the slide was formed after the early Pliocene. To our knowledge, it is the largest submarine landslide ever identified on the Antarctic margin, with approximately 2,300 km^3 of sediments evacuated from the shelf. We propose potential triggers for this slide, including weak layers, fluid and isostatic rebound following ice sheet retreat, although hypothesis relating to the processes has to be tested by direct stratigraphic data. Given the size of the landslide, an improved understanding of whether it was formed during a single event or more gradually during a prolonged interval is critical to evaluate whether Antarctic submarine geohazards may exist in a rapidly changing climates.

Plain Language Summary We present the new discovery of a giant submarine landslide on the east Antarctic margin in front of the Wilkes Subglacial Basin, a major drainage region of the East Antarctic Ice Sheet (EAIS). To our knowledge, it is the largest reported submarine landslide along the Antarctic margin, affecting an area of c. 23, 000 km^2, with approximately 2,300 km^3 of sediments evacuated from the continental shelf, a similar scale to the well-documented Storegga Slide on the Norwegian margin. We propose that the primary factors driving the remobilization of sediment in the form of submarine landslides are linked to the deposition of weak layers, the presence of subseafloor fluids, and rebound of the shelf and the oversteepening of the margin caused by substantial glacier melting in warm climates. Our results suggests that EAIS variance during the Pliocene-Pleistocene ice age cycles has made this region suspectable to submarine landslides, and determining the triggers for such events is critical to understanding future Antarctic submarine geohazards related to the EAIS dynamics under future warming scenarios.

1. Introduction

Submarine landslide extent and processes are poorly constrained on the Antarctic margin, mainly due to the lack of high-resolution bathymetry and seismic data for detailed investigations. Such landslides do exist on many glaciated margins globally, and cover a wide spectrum of dimensions that range from relatively small to massive slides covering thousands of square kilometers (Talling et al., 2014). The scale of large submarine landslides makes them significant as geohazards and posing risks for seafloor infrastructure (Tappin, 2021). One of the largest and best studied submarine landslides is the Storegga Slide, which occurred offshore Norway 8,200 years ago, displacing 3,000 km^3 sediments and generating a large tsunami (Bryn et al., 2005). Mechanically, slides occur when the driving shear stress exceeds the resisting shearing strength, allowing gravitational force to facilitate material transport downslope coupled with internal deformation of the slide. Important factors that contribute to submarine slides are tectonic activity, glacial dynamics, gas hydrates, excess pore pressure and the development of weak layers in marine sediments (Locat et al., 2014; Scarselli, 2020). Past climate variance associated with orbitally paced glacial advances and retreats over glaciated continental margins is proposed to create preconditioning factors for mass slope failures (Gales et al., 2023; Huang et al., 2020; Ottesen et al., 2022). Sediment is transported by ice sheet as a basal bedload to a continental shelf edge, where it is then remobilized into the deep sea by submarine debris flows, landslides and turbidity currents (Huang, Steel, et al., 2022; Pope et al., 2018). Ice sheet dynamics is a primary control on the flux of sediment that reaches the continental shelf edge

(Golledge et al., 2013; Gulick et al., 2024). Glacial retreat cause a dynamic reconfiguration of the continental margin topography, due to isostatic adjustment through time (Stocchi et al., 2013; Whitehouse et al., 2012). This uplifting process may have a stabilizing effect on the ice sheet (Bart & Tulaczyk, 2020; Kingslake et al., 2018), but may also triggered oversteepening and sediment failure on the continental slope (Gales et al., 2023; Huang, Steel, et al., 2022; Huang, Wu, et al., 2022; Hochmuth & Gohl, 2019; Montelli et al., 2017). Triggering factors, spatial distribution and the timing of emplacement of submarine landslides and the relationship with glacial dynamics and climate-driven forces are still not well understood.

An understanding of the location of landslide recurrence, stability of the sea-floor over time, and potential triggers over time is crucial to assess the future geohazards on polar regions, especially proximal to polar coastal populations and submarine infrastructure. In this study, we report the first in-depth analysis of a large-scale submarine landslide on the continental slope in front of the Wilkes Subglacial Basin (WSB), a marine-based sector of the East Antarctic Ice Sheet (EAIS) that was subject to past retreat advance events during the Plio-Pleistocene (Cook et al., 2013; Patterson et al., 2014; Wilson et al., 2018). We use the International Bathymetric Chart of the Southern Ocean v2 data set (Dorschel et al., 2022), multichannel seismic (MCS) data, and correlation to the Integrated Ocean Drilling Program (IODP) Expedition318 sites to characterize and constrain the age of this slide. We aim to contribute to a more profound understanding of the direct (or indirect) influence of ice sheet retreat on sediment failure and slope destabilization processes.

2. Regional Setting

The study area is the continental margin in front of the Cook Ice Shelf and Ninnis Glaciers between 150° and 155°E, 65°and 67°S (Figure 1), which is among the least explored region in Antarctica. The Cook Ice shelf is located on the George V Land Coast (Figure 1) and buttresses the Cook Glacier that drains the ice sheet covering the WSB sector of the EAIS. The WSB is a 400 km-long and ca. 200–600 km-wide tectonic depression (Ferraccioli et al., 2011) that acts as the main sediment source region for glacially discharged material from the Cook and Ninnis Glaciers, among the most active outlet glaciers in East Antarctica. These glaciers discharge about 40 km^3 of ice annually (Miles et al., 2018; Rignot et al., 2011). The ice sheet over the WSB is the largest sector in East Antarctica, grounding (up to 1,500 m) below sea level, making it susceptible to marine ice sheet instabilities in the geological past and the future (Golledge et al., 2017; Wilson et al., 2018).

3. Data and Methods

Sixteen MCS profiles provide the most effective methods of studying submarine landslides as they sample deep into the subsurface, providing spatial resolution and the ability to visualize and estimate both the external and internal volume of deposits. We utilize MCS profiles collected during multiple acquisition cruises on vessels from France, Russia, Australia, USA, Italy and Australia, which are available in the databases of the Antarctic Seismic Data Library System and the Marine Geophysical Data Center.Some seismic lines were reprocessed to remove the sea floor multiple and enhance the signal to noise ratios (Supporting Information S1). Seismic-stratigraphic analyses has been conducted using Petrel and IHS Kingdom softwares.

A detailed analysis of the spatial distribution and chronology of headwall scarps and failures is hindered by the lack of high-resolution seismic data, multibeam and sediment cores in the studied area. Sediments recovered along this margin during IODP Expedition 318 (Escutia et al., 2005) have provided unique chronostratigraphic control for the previously defined seismic units and unconformities of the Wilkes Land margin (Escutia et al., 2005). The age constraint for the seismic horizons (WL-U7 and WL-U8) relevant to this work is obtained via correlation to IODP sites U1361 and U1361 (Figure 1d, Figure S2 in Supporting Information S1). The site U1361contains near-continuous Pliocene and late Miocene sedimentary section from ∼350 to 50 mbsf. A correlation of the existing stratigraphy from the IODP Expedition 318 drill cores (Escutia et al., 2005) to Cook Mega Slide Complex (CMSC) is established through the compilation of a ∼750 km long seismic transect along the continental rise (Figure 1d, Figure S2 in Supporting Information S1), that includes the unpublished MCS profile RAE5507 (Figure 1). A direct correlation of seismic reflectors from IODP Site U1361 to the study area can be made for WL-U7 with high confidence, while WL-U8 is more laterally discontinuous and subject to greater uncertainty. However, the seismic sequence above WL-U8 has a distinct characteristic of unconformity, that can be identified across the margin. Seismic units have been correlated from shelf to rise areas based largely on tracing and projecting unconformities and seismic units from the Site 1,361(Figure 1D, Figure S1 in Supporting

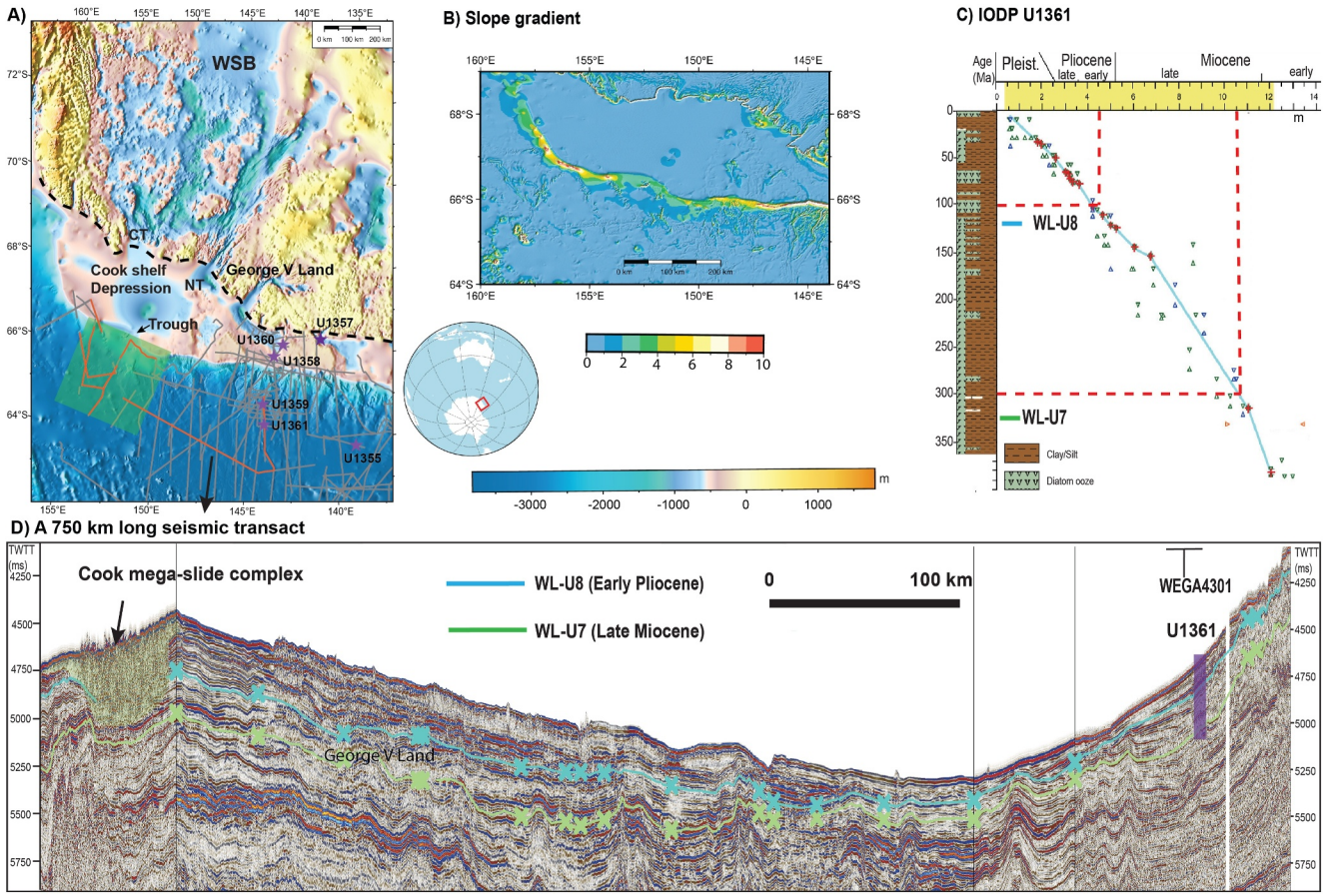

Figure 1. (a) Bathymetric map IBCSO_v2 (Dorschel et al., 2022). Wilkes Subglacial Basin: WSB. The existing seismic data (gray and orange lines), the location of the Integrated Ocean Drilling Program (IODP) Exp318 sites (purple stars), CD = Cook Depression; MT = Mertz Trough; CG = Cook Glacier; NG = Ninnis Glacier; MG = Mertz Glacier. (b) Gradient map of the continental margin, (c) age correlation of the IODP site U1361, Pliocene sediments are characterized by meter-scale alternation of laminated silty clay and bioturbated diatom-rich silty clay. (d) Approximately ~750 km long seismic transect (merged by GA227-4201, GA229-04, RAE5507, GA22902) used to correlate the age information from U1361 to the Cook Mega Slide Complex. WL-U7 and WL-U8 were converted from TWTT to depth at the U1361 site by using the downhole logs for P-wave velocity and density. WL-U7 and WL-U8 lie at 5.03 and 4.78 s TWT, (approximately 300 and 100 mbsf, respectively) and their ages are inferred to be 10.6 and 4.2 Ma respectively (Brinkhuis et al., 2010; Tauxe et al., 2012).

Information S1). Seismic sequences above the WL-U8 unconformity downlap and pinch out at the base of the continental slope, but partially interrupted due to the long transect. The Wilkes Land margin of East Antarctica prograded, with steep forest beds that downlap onto the regional seismic unconformity WL-U8 previously described (Escutia et al., 2005; Santis et al., 2003). At IODP Site U1361, the WL-U8 reflector is correlated as occurring a transition from diatom-rich mudstone deposited during a major glacial retreat in the WSB immediately prior to 4.2 Ma into turbidite mudstones deposited during a subsequent glacial advance (Cook et al., 2013; Patterson et al., 2014) We use a velocity as 1,750 m/s to covert seismic data from time to depth domain based on measured vertical seismic profile in Exp 318. The slides volume can be roughly estimated by determining the affected area and multiplying by the average thickness of the slides, similar to the methods applied by Gales et al. (2023) and Gulick et al. (2024).

4. Results and Interpretation

4.1. Shelf Landforms

The continental shelf adjacent to the WSB is broad, approximately 100–180 km in width (Figure 1a). The inversion of a few airborne gravity data suggest the existence of a depression (the Cook Shelf Depression) on the middle continental shelf up to 500 m deep (Constantino & Tinto, 2023; Frémand et al., 2022). However, the round shaped of this depression has been interpolated from sparse direct bathymetric measurement so the exact

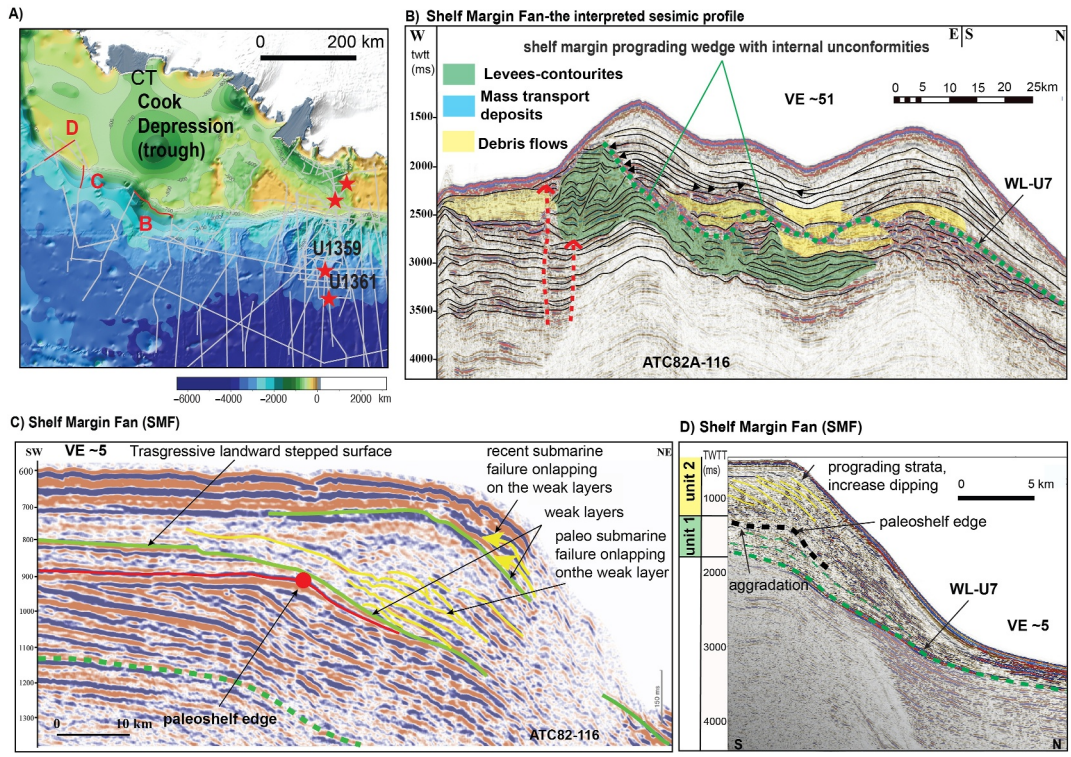

Figure 2. (a) The location of the key seismic profiles. (b) Seismic profile ATC82A-116 showing a strike view of the SMF, (c), (d) and the area of the shelf margin prograding fan (SMF, red line: ATC82A-115). Red dots show the location of present and paleo continental shelf edge. Green shaded areas show sedimentary units deposited during relative high sea level and ice volume minima. Dark lines are glide planes of submarine failure. Yellow lines indicate onlap of deformed sedimentary strata on glide planes. The low amplitude seismic facies in the continental slope indicates the occurrence of gas migrating upward within the sediments.

morphology of the depression is equivocal (Dorschel et al., 2022). Bed Machine compilations (Morlighem et al., 2017) suggests the existence of two other bathymetric depressions (Cook Trough: CT; Ninnis Trough: NT) that are more than 1,000 m deep (Figure 1a), and extended beneath the WSB. Sparse MCS lines reveal that the continental shelf edge is at water depths of between 400 and 700 m. The continental shelf margin has a lobate geometry, with a concave and convex sinuosity at the mouth of the Cook Shelf Depression between 152° and 154°E (Figures 1 and 2).

4.2. Shelf-Margin Fan

A shelf-margin fan, up to 500 m thick, pinches out at the base of the slope between 154° and 157°E (Figure 2b). The fan comprises two units showing subparallel reflections that vary from subhorizontal to gently inclined toward the present and paleo continental shelf edge (Figure 2b). The upper Unit 2 is characterized by inclined reflections downlapping onto Unit 1 and sharply truncated by flat and sub-horizontal reflections on the top (Figure 2c). During the build-up of the shelf-margin fan, the continental slope gradually steepened and the paleoshelf edge prograded by approximately 3 km during the deposition of Unit 1 (Figure 2b). An E-W MCS line on the upper continental slope (Figures 2c and 2d) shows a strike view of the internal fan architecture. This sector of the slope is characterized by mounded features that are internally stratified (green shaded seismic unit), below WL-U7 (green dashed line in Figure 2c). The mounded feature is onlapped and interlayered with a chaotic lens (yellow shaded seismic unit), subdivided into packages by angular unconformities. The N-S segment of the seismic profile (right Figure 2c) shows a dip view of the fan seaward termination that downlaps northwards onto the stratified and chaotic lower unit.

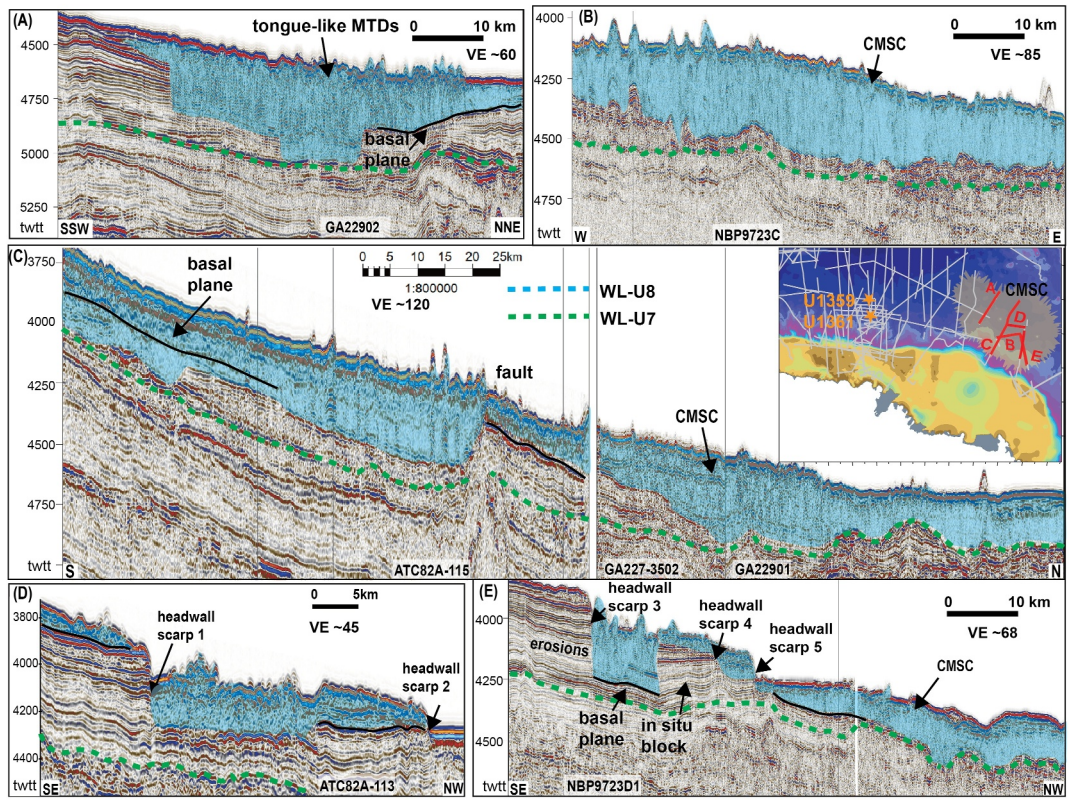

Figure 3. Cook Mega Slide Complex imaged by the seismic lines. The black line marks the base of the acoustic opaque facies interpreted as mass failure planes. Black dashed line indicates headwall scarps (1–5). (a) CMSC is imaged by the seismic line GA22902; (b) CMSC is imaged by the seismic line NBP9723C; (c) CMSC is imaged by the seismic lines ATC82A-115, GA227-3502, GA22901; (d) CMSC is imaged by the seismic line ATC82A-113, scarp 1 and scarp 2 are observed; (e) CMSC is imaged by the seismic line NBP9723D1, scarp 3–5 are observed.

4.3. Cook Mega Slide Complex (CMSC)

The MCS lines reveal the occurrence of an acoustic semitransparent or chaotic package with the external shape of a lens or a wedge thinning downslope. It has a thickness of up to 250-milliseconds (ms) corresponding to ca.220 m thickness considering an averaged interval velocity of 1750 m/s (Figure 3). The package is located in the concave and lees steep sector of the continental margin extends over 300 km along the continental slope in water depths between 2,500 and 3,000 m (Figures 3a–3c). The sea floor represents the upper surface of the package, while the lower surface is characterized either by a strong amplitude reflection that truncates stratified units (Figures 3a, 3c, and 3e) or an irregular, locally stepped, ramp and flat type geometry (Figures 3a, 3b, and 3e) on MCS lines. These observations are consistent with established criteria for identifying submarine landslides (Bull et al., 2009; Hampton et al., 1996), and we refer here to this semitransparent/chaotic package as the CMSC.

The morphology of the base of the CMSC as defined above is consistent as a failure, glide planes, which are common features in areas with documented mass movements (Baeten et al., 2014). Steep morphological steps correspond to headwall scarps (headwall scarp 1–5, Figure 3). Their height range from 150 m (scarp 1 in Figures 3d) to 60 m (scarp 4 in Figure 3e). The headwall scarps display inclinations of 5–15°, and truncate the adjacent strata. Some headwall scarps intersect the sea floor, while others appear to be buried (Figure 3e). The headwall scarps represent the breakaway planes from where sediments detached and were transported by gravity-driven processes down to the base of the slide (Figures 3c and 3e).

The CMSC lying seaward of the headwall scarps represents the sediment material that evacuated away as submarine landslides from the upper to the lower slope, sliding over glide planes and finally depositing at the failure foot. The orientation of the scarp propagations and failures, and the location of the deposited sediments, suggest that the gross transport direction of the slides was from south to north (Figure 3).

5. Discussion

The total volume of the CMSC is more than 2,300 km^3; based on a minimum length estimation of 175 km, a width of 50 km, and thickness of 0.27 km. Such a volume is comparable in size with the Storegga Slide along the Norwegian slope (maximum volume of 3,200 km^3; Bryn et al., 2005), and the Mafia mega-slide (maximum volume > 2,500 km^3) in the Indian Ocean (Maselli et al., 2020). Tsunamis can be generated by submarine landslides through the vertical displacement of the sea floor during landslide movement. The Storegga slides involved an estimated 290 km length of coastal shelf, with a total volume of 3,500 km^3 of debris, which caused a paleo tsunami in the North Atlantic Ocean, with estimated run-up heights of around 10–20 m on the Norwegian coast, over 30 m in Shetland Islands Coast. Given an estimated volume of 2,300 km^3 of CMSC, there is a significant paleotsunami potential on the coast of the Cook shelf as well, although detailed tsunami modeling would be required to quantify such a hazard.

5.1. Possible Triggers

The failures possible occurred as multiple events and retrogressive movements (Figure 3), which would mitigate some of the tsunami risk potential noted above, but a precise dating is challenging due to the lack of direct constraints in the CMCS area. Direct dating is crucial for accurately estimating frequencies, recurrence rates and identify triggers (Clare et al., 2014; Urlaub et al., 2013). The identification of the WL-U7 and WL-U8 regional seismic unconformities in the CMCS area, tied to the IODP Expedition 318 drill sites (Figure 2) indicates that the CMSC likely formed after the early Pliocene (Figure 1, Figures S1 and S2 in Supporting Information S1).

Sediment records from Sites U1358 on the adjacent Adélie Land continental shelf and U1361 in the continental rise, deposited between 5.3 and 3.3 million years ago, consist of alternating diatom-rich silty clay layers and diatom-poor clay layers with silt laminations (Cook et al., 2013; Orejola et al., 2014). The diatom-rich units correlate with higher Ba/Al ratios, suggesting multiple extended periods of increased biological productivity related to less sea ice, and warmer spring and summer sea surface temperatures. The clay-rich units were instead deposited in colder periods, with more extensive ice sheet cover. A similar glacial and interglacial sediment layering is observed in Ross Sea Plio-Pleistocene sequences (McKay et al., 2019; Seidenstein et al., 2024), where the diatom-rich, low-density strata acted as weak layers, favoring the sliding of denser, glacial clay- and gravel rich sediments (Gales et al., 2023). In the case of the Ross Sea, glide planes were drilled at the IODP site U1523 and identified as parallel, seaward inclined continuous reflectors on seismic profiles, and transitions from diatom-rich to gravel rich sediment.

Potential glide planes can also be identified on the seismic profiles (e.g., NBP97-23A, see Supporting Information S1) located in the eastern sector of the CMCS. The seismic reflection (green reflectors in Figure 1, Figure S1 in Supporting Information S1) can be traced from the continental shelf to the slope, where they are onlapped by deformed, discontinuous seismic signals. Some reflections cut subhorizontal layers, possibly representing retrogressive scarp-failure features affecting the paleoshelf edge. Based on the correlation to the unconformity WL-U8, we can infer that weak layers acting as glide planes of the most recent CMSC submarine failures have a Plio-Pleitocene age (Figures S1 and S2 in Supporting Information S1). At Site U1361, seismic surface WL-U8 correlates with a transition at 4.2 Ma from diatom-rich muds, interpreted as a major deglaciation of WSB, to laminated (diatom-poor) muds (Cook et al., 2013; Patterson et al., 2014). This stratigraphic configuration has been shown in other polar regions as pre-condition slope for failure, and trigger large submarine landslides (Karstens et al., 2023).

The increased sediment flux during glacial maxima to the continental shelf edge, as evidenced by the formation of the shelf-margin fan (Figures 2c and 2d), is a common pre-conditioning factor of submarine slope failure (Gulick et al., 2024; Ten Brink et al., 2016). The upper-slope collapse inside the shelf-margin fan and CMSC (Figures 2–4) could also be affected by uplift during post-glacial unloading and bedrock rebound (Figure 4). The massive deglaciation and retreat of the EAIS could have led to excess pore pressure when a compressible pore fluid is present. The high excess pore pressures promote the excess pore fluid migration toward the slope, where an increase in the overpressure ratio will be generated. In the MCS profiles, we have observed pipe-like structure formation, with blanking and seismic reflections anomaly that may indicate conduits of fluid migration or free gas (Figure 4c). The velocity analysis from reprocessing the seismic profile (Figure 4c) shows an inversion at 2–2.25 s (twtt) at CDPs 4,404–4,406 that indicates the occurrence of gas trapped within the sediment in the continental slope (Figure 4c). On the other hands, a very low velocity within 0.5 s (twtt) on the upper slope (CDP 4,500–

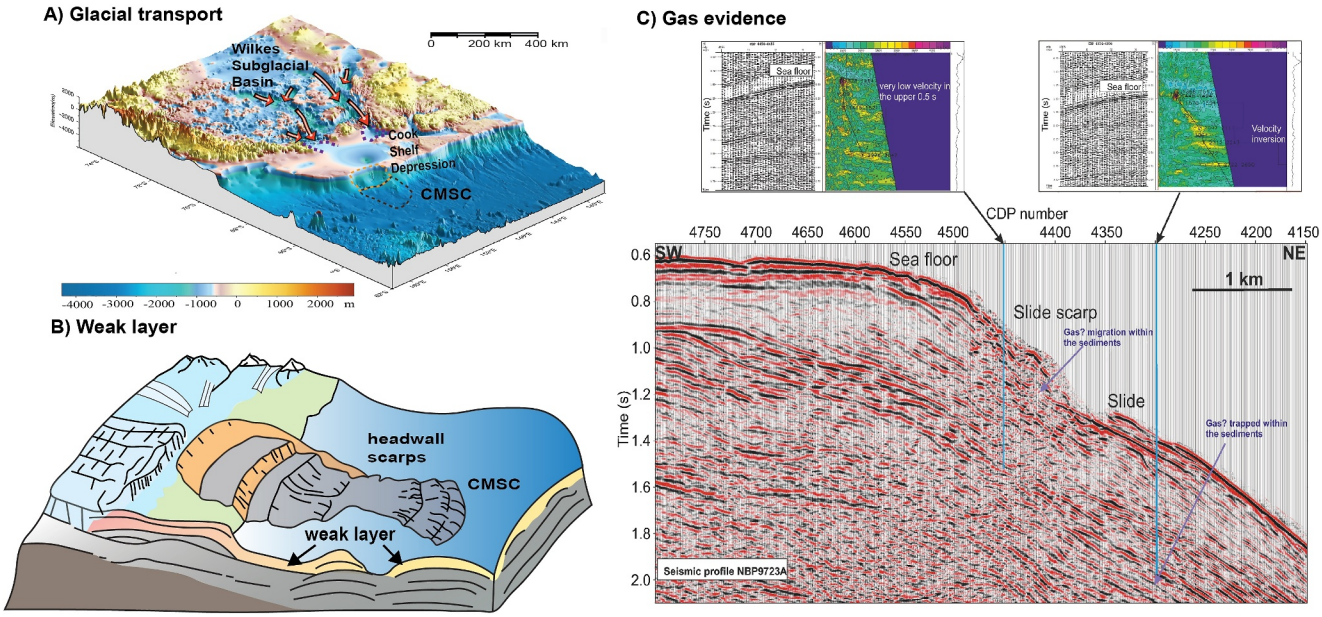

Figure 4. Schematic maps of (a) inferred source and pathways of the sediments; (b) a sketch of Cook Mega Slide Complex; (c) The velocity analysis from reprocessing the seismic profile NBP9723A shows an inversion at 2–2.25 s (twtt) at CDPs 4,404–4,406, and a very low velocity within 0.5 s (twtt) on the upper slope (CDP 4,500–4,380).

4,380) (Figures 1 and 4c). Here the continental slope is cut by scarps, suggesting that the release of gas, migrating upward within the sediments could have favored the submarine slope sliding. Identifying potential fluid-escape pathways for past or future releases of fluids or gases (including methane) from unstable slope sediments has important implications for ocean chemistry and the sudden increase in atmospheric greenhouse gases.

6. Conclusions

We present the first evidence of a large submarine failure, the CMSC, affecting the East Antarctic continental slope, in the Plio-Pleistocene, by using a grid of seismic profiles. The failure occurred in the region in front of the Cook and Ninnis Glaciers, which are the major drainage glaciers of the WSB, and we proposed the advance and retreat of these glaciers during Pliocene resulted into an outer continental shelf stratigraphy that was prone to slope failure. This stratigraphy include deposition of weak layers, acting as potential glide planes, made of soft diatom-rich sediments, locally trapping gas, deposited during past ice sheet minimum expansions, and alternated with compacted and denser glacial mud layers. The occurrence of the CMSC and its formation involving multiple events suggests that this sector of the Antarctic margin has been highly dynamic, with periods of increased ice extent, but also extensive and rapid retreat in response to warming climate since the early Pliocene and up to recent times. Such "preconditioning" in outer continental shelf stratigraphy have been noted in the Ross Sea, which also demonstrated highly dynamic marine-based ice sheet variances (Gales et al., 2023). The results have implications for future behavior and sensitivity of this and other sectors of the AIS where there have been past marine-based ice sheet variances and creating similar alternations of weak and cohesive layers–and could be prone to future slope failure events. Attention should be paid to regions with large thickness of sediments still accumulated at the Antarctic continental margin adjacent to large marine-based subglacial basins–and where instability may be threatened by further climate warming and sea level rise. Although we discuss potential triggers for landslide occurrence, we acknowledge these are currently speculative and require validation via direct sampling. Improved knowledge of submarine landslide triggers of Antarctica is needed to identify and mitigate potential geohazard risks for Antarctic infrastructure and Southern Hemisphere populations.

Data Availability Statement

The reflection seismic data used in this study is freely available through the Antarctic SDLS under https://sdls.ogs.trieste.it. The reflection seismic data sets shown in this study (GA227-4201, GA227-3502, GA22901, GA22902,

GA229-04, RAE5507, ATC82A-116, ATC82A-115, ATC82A-113,NBP9723A, NBP9723B, NBP9723D1) can be downloaded from the SDLS via the "Access Data" tab or by searching the database.

Acknowledgments
XH acknowledges the support of the National Natural Science Foundation of China (42476270), the Pioneer Hundred Talents Program (Y910091001) Chinese Academy of Sciences (CAS), LD acknowledges funding from the Italian National Antarctic Research Program (PNRA19_00022 project). RM acknowledges support from MBIE Antarctic Science Platform contract ANTA1801.

References

Baeten, N. J., Laberg, J. S., Vanneste, M., Forsberg, C. F., Kvalstad, T. J., Forwick, M., et al. (2014). Origin of shallow submarine mass movements and their glide planes—Sedimentological and geotechnical analyses from the continental slope off northern Norway. *Journal of Geophysical Research: Earth Surface*, *119*(11), 2335–2360. https://doi.org/10.1002/2013jf003068

Bart, P. J., & Tulaczyk, S. (2020). A significant acceleration of ice volume discharge preceded a major retreat of a West Antarctic paleo–ice stream. *Geology*, *48*(4), 313–317. https://doi.org/10.1130/G46916.1

Brinkhuis, H., Dotti, C. E., Klaus, A., Fehr, A., Williams, T., Bendle, J., et al. (2010). Wilkes land glacial history Cenozoic East Antarctic ice sheet evolution from Wilkes Land margin sediments. https://doi.org/10.2204/iodp.pr.318.2010

Bryn, P., Berg, K., Forsberg, C. F., Solheim, A., & Kvalstad, T. J. (2005). Explaining the Storegga slide. *Marine and Petroleum Geology*, *22*(1–2), 11–19. https://doi.org/10.1016/j.marpetgeo.2004.12.003

Bull, S., Cartwright, J., & Huuse, M. (2009). A review of kinematic indicators from mass-transport complexes using 3D seismic data. *Marine and Petroleum Geology*, *26*(7), 1132–1151. https://doi.org/10.1016/j.marpetgeo.2008.09.011

Clare, M. A., Talling, P. J., Challenor, P., Malgesini, G., & Hunt, J. (2014). Distal turbidites reveal a common distribution for large (>0.1 km^3) submarine landslide recurrence. *Geology*, *42*(3), 263–266. https://doi.org/10.1130/G35160.1

Constantino, R. R., & Tinto, K. J. (2023). Cook ice shelf and Ninnis glacier tongue bathymetry from inversion of operation ice bridge airborne gravity data. *Geophysical Research Letters*, *50*(11), e2023GL103815. https://doi.org/10.1029/2023GL103815

Cook, C. P., van de Flierdt, T., Williams, T., Hemming, S. R., Iwai, M., Kobayashi, M., et al. (2013). Dynamic behaviour of the East Antarctic ice sheet during Pliocene warmth. *Nature Geoscience*, *6*(9), 765–769. https://doi.org/10.1038/ngeo1889

De Santis, L., Brancolini, G., & Donda, F. (2003). Seismo-stratigraphic analysis of the Wilkes Land continental margin (East Antarctica): Influence of glacially driven processes on the Cenozoic deposition. *Deep-Sea Research Part II Topical Studies in Oceanography*, *50*(8–9), 1563–1594. https://doi.org/10.1016/s0967-0645(03)00079-1

Dorschel, B., Hehemann, L., Viquerat, S., Warnke, F., Dreutter, S., Tenberge, Y. S., et al. (2022). The international bathymetric chart of the Southern Ocean version 2. *Scientific Data*, *9*(1), 1–13. https://doi.org/10.1038/s41597-022-01366-7

Escutia, C., De Santis, L., Donda, F., Dunbar, R. B., Cooper, A. K., Brancolini, G., & Eittreim, S. L. (2005). Cenozoic ice sheet history from East Antarctic Wilkes Land continental margin sediments. *Global and Planetary Change*, *45*(1), 51–81. https://doi.org/10.1016/j.gloplacha.2004.09.010

Ferraccioli, F., Finn, C. A., Jordan, T. A., Bell, R. E., Anderson, L. M., & Damaske, D. (2011). East Antarctic rifting triggers uplift of the gamburtsev mountains. *Nature*, *479*(7373), 388–392. https://doi.org/10.1038/nature10566

Frémand, A. C., Bodart, J. A., Jordan, T. A., Ferraccioli, F., Robinson, C., Corr, H. F., & Vaughan, D. G. (2022). British Antarctic survey's aerogeophysical data: Releasing 25 years of airborne gravity, magnetic, and radar datasets over Antarctica. *Earth System Science Data Discussions*, *2022*, 1–49. https://doi.org/10.5194/essd-14-3379-2022

Gales, J. A., McKay, R. M., De Santis, L., Rebesco, M., Laberg, J. S., Shevenell, A. E., et al. (2023). Climate-controlled submarine landslides on the Antarctic continental margin. *Nature Communications*, *14*(1), 2714. https://doi.org/10.1038/s41467-023-38240-y

Golledge, N. R., Levy, R. H., McKay, R. M., Fogwill, C. J., White, D. A., Graham, A. G. C., et al. (2013). Glaciology and geological signature of the last glacial maximum Antarctic ice sheet. *Quaternary Science Reviews*, *78*, 225–247. https://doi.org/10.1016/j.quascirev.2013.08.011

Golledge, N. R., Thomas, Z. A., Levy, R. H., Gasson, E. G., Naish, T. R., McKay, R. M., et al. (2017). Antarctic climate and ice-sheet configuration during the early Pliocene interglacial at 4.23 Ma. *Climate of the Past*, *13*(7), 959–975. https://doi.org/10.5194/cp-13-959-2017

Gulick, S. P., Reece, R. S., Sawyer, D. E., Christeson, G. L., & Horton, B. K. (2024). Effect of seismicity and tectonic-glacial interactions on submarine megaslides. *Geophysical Research Letters*, *51*(7), e2024GL108374. https://doi.org/10.1029/2024gl108374

Hampton, M. A., Lee, H. J., & Locat, J. (1996). Submarine landslides. *Reviews of Geophysics*, *34*(1), 33–59. https://doi.org/10.1029/95RG03287

Hochmuth, K., & Gohl, K. (2019). Seaward growth of Antarctic continental shelves since establishment of a continent-wide ice sheet: Patterns and mechanisms. *Palaeogeography, Palaeoclimatology, Palaeoecology*, *520*, 44–54. https://doi.org/10.1016/j.palaeo.2019.01.025

Huang, X., Bernhardt, A., De Santis, L., Wu, S., Leitchenkov, G., Harris, P., & O'Brien, P. (2020). Depositional and erosional signatures in sedimentary successions on the continental slope and rise off Prydz Bay, East Antarctica–Implications for Pliocene paleoclimate. *Marine Geology*, *430*, 106339. https://doi.org/10.1016/j.margeo.2020.106339

Huang, X., Steel, R., & Larter, R. D. (2022). Late Eocene signals of oncoming Icehouse conditions and changing ocean circulation, Antarctica. *Earth and Planetary Science Letters*, *600*, 117885. https://doi.org/10.1016/j.epsl.2022.117885

Huang, X., Wu, S., De Santis, L., Wang, G., & Hernández-Molina, F. J. (2022). Deep water sedimentary processes in the Enderby Basin (East Antarctic margin) during the Cenozoic. *Basin Research*, *34*(6), 1917–1935. https://doi.org/10.1111/bre.12690

Karstens, J., Haflidason, H., Berndt, C., & Crutchley, G. J. (2023). Revised storegga slide reconstruction reveals two major submarine landslides 12,000 years apart. *Communications Earth & Environment*, *4*(1), 55. https://doi.org/10.1038/s43247-023-00710-y

Kingslake, J., Scherer, R. P., Albrecht, T., Coenen, J., Powell, R. D., Reese, R., et al. (2018). Extensive retreat and re-advance of the West Antarctic ice sheet during the holocene. *Nature*, *558*(7710), 430–434. https://doi.org/10.1038/s41586-018-0208-x

Locat, J., Leroueil, S., Locat, A., & Lee, H. (2014). Weak layers: Their definition and classification from a geotechnical perspective. In S. Krastel (Ed.), et al. (Eds.), *Submarine mass movements and their consequences*, *Advances in natural and technological hazards Research* (Vol. 37, pp. 3–12). Springer. https://doi.org/10.1007/978-3-319-00972-8_1

Maselli, V., Iacopini, D., Ebinger, C. J., Tewari, S., de Haas, H., Wade, B. S., et al. (2020). Large-scale mass wasting in the western Indian Ocean constrains onset of East African rifting. *Nature Communications*, *11*(1), 3456. https://doi.org/10.1038/s41467-020-17267-5

McKay, R. M., De Santis, L., & Kulhanek, D. K. (2019). Ross sea West Antarctic ice sheet history. *Proceedings of the International Ocean Discovery Program*, *374*. https://doi.org/10.14379/iodp.proc.374

Miles, B. W., Stokes, C. R., & Jamieson, S. S. (2018). Velocity increases at cook glacier, East Antarctica, linked to ice shelf loss and a subglacial flood event. *The Cryosphere*, *12*(10), 3123–3136. https://doi.org/10.5194/tc-12-3123-2018

Montelli, A., Dowdeswell, J. A., Ottesen, D., & Johansen, S. E. (2017). Ice-sheet dynamics through the quaternary on the mid-Norwegian continental margin inferred from 3D seismic data. *Marine and Petroleum Geology*, *80*, 228–242. https://doi.org/10.1016/j.marpetgeo.2016.12.002

Morlighem, M., Williams, C. N., Rignot, E., An, L., Arndt, J. E., Bamber, J. L., et al. (2017). BedMachine v3: Complete bed topography and ocean bathymetry mapping of Greenland from multibeam echo sounding combined with mass conservation. *Geophysical Research Letters*, *44*(21), 11–51. https://doi.org/10.1002/2017GL074954

Orejola, N., Passchier, S., & Expedition, I. O. D. P. (2014). Sedimentology of lower Pliocene to upper Pleistocene diamictons from IODP site U1358, Wilkes land margin, and implications for East Antarctic ice sheet dynamics. *Antarctic Science*, *26*(2), 183–192. https://doi.org/10.1017/S0954102013000527

Ottesen, D., Batchelor, C. L., Bjarnadóttir, L. R., Wiberg, D. H., & Dowdeswell, J. A. (2022). Glacial landforms reveal dynamic ice-sheet behaviour along the mid-Norwegian margin during the last glacial-deglacial cycle. *Quaternary Science Reviews*, *285*, 107462. https://doi.org/10.1016/j.quascirev.2022.107462

Patterson, M. O., McKay, R., Naish, T., Escutia, C., Jimenez-Espejo, F. J., Raymo, M. E., et al. (2014). Orbital forcing of the East Antarctic ice sheet during the Pliocene and early Pleistocene. *Nature Geoscience*, *7*(11), 841–847. https://doi.org/10.1038/ngeo2273

Pope, E. L., Talling, P. J., & Cofaigh, C. Ó. (2018). The relationship between ice sheets and submarine mass movements in the Nordic seas during the quaternary. *Earth-Science Reviews*, *178*, 208–256. https://doi.org/10.1016/j.earscirev.2018.01.007

Rignot, E., Mouginot, J., & Scheuchl, B. (2011). Ice flow of the Antarctic ice sheet. *Science*, *333*(6048), 1427–1430. https://doi.org/10.1126/science.1208336

Scarselli, N. (2020). Submarine landslides–architecture, controlling factors and environments. A summary. In *Regional geology and tectonics* (pp. 417–439). Elsevier. https://doi.org/10.1016/B978-0-444-64134-2.00015-8

Seidenstein, J. L., Leckie, R. M., McKay, R., De Santis, L., Harwood, D., & Expedition, I. O. D. P. (2024). Pliocene–Pleistocene warm-water incursions and water mass changes on the Ross Sea continental shelf (Antarctica) based on foraminifera from IODP Expedition 374. *Journal of Micropalaeontology*, *43*(2), 211–238. https://doi.org/10.5194/jm-43-211-2024

Stocchi, P., Escutia, C., Houben, A. J., Vermeersen, B. L., Bijl, P. K., Brinkhuis, H., et al. (2013). Relative sea-level rise around East Antarctica during Oligocene glaciation. *Nature Geoscience*, *6*(5), 380–384. https://doi.org/10.1038/ngeo1783

Talling, P. J., Clare, M. L., Urlaub, M., Pope, E., Hunt, J. E., & Watt, S. F. (2014). Large submarine landslides on continental slopes: Geohazards, methane release, and climate change. *Oceanography*, *27*(2), 32–45. https://doi.org/10.5670/oceanog.2014.38

Tappin, D. R. (2021). Submarine landslides and their tsunami hazard. *Annual Review of Earth and Planetary Sciences*, *49*(1), 551–578. https://doi.org/10.1146/annurev-earth-063016-015810

Tauxe, L., Stickley, C. E., Sugisaki, S., Bijl, P. K., Bohaty, S. M., Brinkhuis, H., et al. (2012). Chronostratigraphic framework for the IODP expedition 318 cores from the Wilkes land margin: Constraints for aleoceanographic reconstruction. *Paleoceanography*, *27*(2), PA2214. https://doi.org/10.1029/2012PA002308

Ten Brink, U. S., Andrews, B. D., & Miller, N. C. (2016). Seismicity and sedimentation rate effects on submarine slope stability. *Geology*, *44*(7), 563–566. https://doi.org/10.1130/G37866.1

Urlaub, M., Talling, P. J., & Masson, D. G. (2013). Timing and frequency of large submarine landslides: Implications for understanding triggers and future geohazard. *Quaternary Science Reviews*, *72*, 63–82. https://doi.org/10.1016/j.quascirev.2013.04.020

Whitehouse, P. L., Bentley, M. J., Milne, G. A., King, M. A., & Thomas, I. D. (2012). A new glacial isostatic adjustment model for Antarctica: Calibrated and tested using observations of relative sea-level change and present-day uplift rates. *Geophysical Journal International*, *190*(3), 1464–1482. https://doi.org/10.1111/j.1365-246X.2012.05557.x

Wilson, D. J., Bertram, R. A., Needham, E. F., Flierdt, T. van de, Welsh, K. J., McKay, R. M., et al. (2018). Ice loss from the East Antarctic ice sheet during late pleistocene interglacials. *Nature*, *561*(7723), 383–386. https://doi.org/10.1038/s41586-018-0501-8